



Diagnosis and precise localization of cardiomegaly disease using U-NET

Abdelilah Bouslama^{*}, Yassin Laaziz, Abdelhak Tali

Abdelmalek Essaadi University, LabTIC, ENSA, Tangier, Morocco

ARTICLE INFO

Keywords:

CXR
Cardiomegaly
CNN
AHE
U-Net

ABSTRACT

This study examines an end-to-end technique which uses a Deep Convolutional Neural Network U-Net based architecture to detect Cardiomegaly disease. The learning phase is achieved by using Chest X-ray images extracted from the “ChestX-ray8” open source medical dataset. The Adaptive Histogram Equalization (AHE) method is deployed to enhance the contrast and brightness of the original images. These latter are compressed before undergoing a training stage to optimize computation time. By this method, we obtained a diagnostic accuracy greater than 93%, which outperforms published results for recognizing Cardiomegaly disease. In addition, with U-Net, precise localization of Cardiomegaly is possible, which is not the case in previous works.

1. Introduction

X-ray radiography is one of the simplest and most commonly available techniques that can be utilized for the detection and diagnosis of many diseases. Consequently, a large quantity of radiographic images and reports are generated and stored daily in hospital archives around the world. These archives constitute a considerable and valuable source of information, which remains minimally exploited because of the lack of means of automation of the image analysis process.

One of the solutions considered to solve this problem and give a value-added to these archives lies in the use of artificial intelligence, and in particular deep learning techniques, which have proved their effectiveness for objects detection [1] and image segmentation [2].

Among these techniques, Convolutional Neural Networks (CNN) have shown excellent performance in computer vision and machine learning. The medical field is one of the areas in which this technology has attracted a great deal of interest, which has manifested itself in numerous published articles. In particular, research has been conducted to develop CNN models capable of diagnosing thoracic diseases, including lung nodules at Computed Tomography (CT scan) [3], pleural effusion and cardiomegaly [4], pulmonary tuberculosis [5] and Pneumonia [6]. In all these works a high detection accuracy rate lying between 88% and 91% was reported. Nevertheless, much work remains to be performed for example in the field of the complexity of algorithms, learning methods and the use of more or less large databases, which are the main vectors for the development of efficient and inexpensive techniques for automating the medical analysis process from Chest X-rays (CXR).

This work focuses on Cardiomegaly disease, a medical term used to refer to cardiac hypertrophy. We have fixed three main objectives: the first is to achieve automatic detection of this disease in a CXR image, the second is to determine accurately its location in the image, and the third consists to improve the detection accuracy reported in other works.

For this purpose, we have developed a new CNN algorithm based on U-Net, in which the learning phase is performed using CXR images extracted from the open source medical database “ChestX-ray8” [7]. It should be noted that although the images used have good resolutions of (1024×1024) pixels, it has been found that the contrast for some extracted images is very low, which makes it difficult to make a correct diagnosis of the disease, and this fact impacts directly the accuracy of the detection. So we set up a pre-treatment step before using the “ChestX-ray8” images in order to improve their quality. This treatment is based on a well-known method called AHE (Adaptive Histogram Equalization) [8] that allows to increase the contrast and to spread out the most frequent intensity values in an image.

Using the “ChestX-ray8” database we have identified 1010 images dedicated to Cardiomegaly disease. Nevertheless, it is hard to work with such a great number of images in deep learning processes, especially if the images are kept at their original size. One of our main objectives being to propose a simple treatment model, we opted to undergo a phase of compression to the images. This compression was ensured without altering the quality nor the content of images by using HDF5, which allows to manipulate digital data quantities of several terabytes by preparing, categorizing and marking multidimensional arrays in a single file.

Another difficulty with the “ChestX-ray8” dataset is the absence of

^{*} Corresponding author.

E-mail address: bo.abdelilah@gmail.com (A. Bouslama).

<https://doi.org/10.1016/j.imu.2020.100306>

Received 13 December 2019; Received in revised form 10 February 2020; Accepted 2 March 2020

Available online 20 March 2020

2352-9148/© 2020 The Authors.

Published by Elsevier Ltd.

This is an open access article under the CC BY-NC-ND license

(<http://creativecommons.org/licenses/by-nc-nd/4.0/>).

image masks, which leads to a poorly supervised learning problem. This is why we manually created masks for over a thousand images.

For the treatment phase, we used a particular architecture CNN namely U-Net, which uses a Fully Convolutional Network.

Model, giving better segmentation in medical imaging [9]. This proposed CNN model reaches a diagnosis accuracy greater than 93%, which is better than published results for recognizing Cardiomegaly disease. In addition, with U-Net, precise localization of Cardiomegaly is possible, which is not the case for the previous works.

The remainder of the paper can be summarized as follows. In the second section, we give a brief survey of recent works on the application of deep learning for medical image analysis. Then, in section three, we develop the different steps for the pre-treatment of images, starting by explaining the reasons for choosing the “ChestX-ray8” dataset, describing the different steps to extract Cardiomegaly images, and the operations of optimization and compression of images. In the fourth section we present in detail the different phases of the implementation of our U-Net based CNN algorithm. Finally, section five gives the results of implementation of this algorithm for Cardiomegaly disease detection from CXR images.

2. Related works

Previously published work has reported very high detection success rates; as in Ref. [10], where the authors employed a CNN based on ImageNet to identify different pathologies in CXR images and obtained a rate of 89%. In another work [11], the authors presented a new architecture named DualNet that processes simultaneously both frontal and lateral CXR images. In this case an accuracy of 91% has been reported, but the authors used a large set of MIMIC-CXR data (thousands of images). In Ref. [12], the authors achieved an accuracy of 92%, but this was reached using pre-configured and heavy models such as ResNet-101.

In another work, a team from Taishan Medical University [13], developed an automatic method, based on a CNN algorithm, to identify a patient’s position and body region from digital radiographic images. For this aim, they have used only frequency curve classification and gray matching; however, in order to achieve the 90% prediction accuracy, more than 7000 images were necessary.

Otherwise, recent research [14] enabled to classify the 8 diseases present in the ChestX-ray8 database. Nevertheless, the method uses heavy and pre-trained models such as ResNet-101 and ImageNet and can’t locate the disease inside the CXR. Another approach to use the concept of deep learning for detection pathologies from CXR was implemented by applying a preconfigured model, intended for generic visual recognition [15]. Nevertheless, the model is limited to detection and doesn’t allow positioning of the disease in the CXR.

In this paper we are interested not only in detecting Cardiomegaly disease and to enhance detection precision with respect to previous works, but we aim as well to locate precisely the disease inside the CXR and to propose an algorithm using a small set of data for training. The U-Net based CNN algorithm we developed enabled us to obtain a high detection precision of between 93 and 94%, from a small dataset in the training phase. Up to now our method gives good results compared to cited works [10,11], that used heavy and preconfigured models (VGG16, VGG19 and ResNet). To the best of our knowledge, this is the first time such a procedure is reported, offering precise detection of Cardiomegaly disease, but also enabling to locate it inside the CXR images. The different stages of implementation of our model will be developed below.

3. Cardiomegaly disease

3.1. Pre-processing treatment

3.1.1. ChestX-ray8 dataset

“ChestX-ray8” is an open-source medical database consisting of 108,948 frontal views of CXR images of 32,717 unique patients, comprising classified images of 8 popular diseases. “ChestX-ray8” was launched by teams from the Department of Radiology and Imaging Sciences, National Library of Medicine, and National Institutes of Health, Bethesda A ELIMINER [7]. This dataset is available and shared for research purposes and for performance evaluation of different computer aided detection systems.

We extract first the Cardiomegaly images from the Excel files offered by “ChestX-ray8” dataset, using a basic Python script that separates files, based on their label, in separate folders. This allowed us to extract 1010 images corresponding to Cardiomegaly. Nevertheless, these 1024×1024 resolution images are given without any masks or annotations showing the position of disease. Thus, they have to be preprocessed before applying Deep Learning technique.

3.1.2. Optimization of image contrast

Image contrast enhancement is used widely in digital image processing; the main idea behind this technique is to show hidden details that can contain interesting information in the image.

One of the most popular techniques is HE (Histogram Equalization), which focuses on increasing the intensity of the image by enhancing the contrast. This is accomplished by applying all possible values of red, green and blue channels in each pixel. It shows good results in colorized images but it is very limited with grayscale ones. For these images it is more interesting to use the AHE method (Adaptive Histogram Equalization) [16] instead of HE, which takes each image and applies multiple histogram operations to differentiate between pixel levels of each image region. Nevertheless, in this work, we used a modified version of AHE called Low Contrast AHE Method (LC-AHE), introduced by a team at the Medical Image Display Research Group at the University of North Carolina [17]. This technique takes a small region of the image, called the contextual region, and modifies the brightness of each of its pixels according to the intensity levels of the neighboring pixels. This increases the cumulative distribution function (CDF), which improves the sharpness of the image in areas of low intensity pixels.

The LC-AHE process is based on five main steps [18]:

1. Determine each grid and its points on the image (Starting from the top-left corner).
2. Mapping calculation of points on each grid.
3. Finding the four closest neighboring grid points of each pixel.
4. Interpolating among these pixel values to obtain the mapping at the current pixel location. Map this intensity to the range [min:max] and put it in the output image.
5. Mapping to each pixel location the intensity based on range of minimum and maximum values.

Fig. 1 compares the histograms and CDFs of a Cardiomegaly image in the following three cases: untreated image (a), image processed with the HE method (b) and image treated with LC-AHE (c).

Obviously image contrast in case “c” has been significantly improved as a result of sharpening. This is confirmed by the increase in the histogram of the image in a much wider range of gray levels and also by the improvement of the cumulative distribution function, going from case (a) to (c). The LC-AHE treatment is therefore more efficient than the conventional AHE treatment to improve quality of image.

3.1.3. Compression of the extracted images

The idea of working directly with the 1010 images with a resolution of 1024×1024 each was not practical. Indeed, the fact of loading each

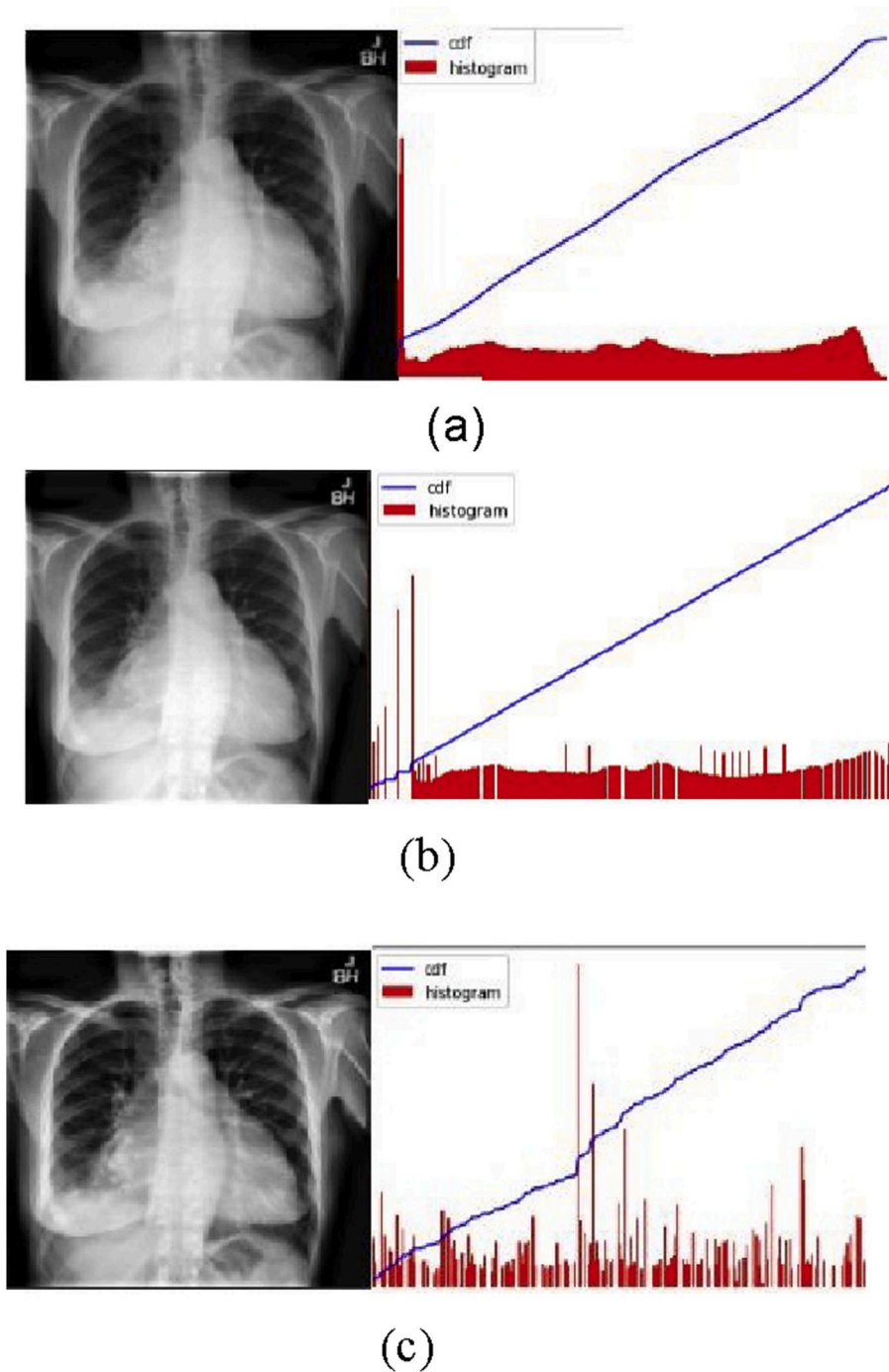


Fig. 1. Histogram and CDF of a Cardiomegaly image; (a) untreated image (b) HE treated image, (c) LC-AHE treated image.

image separately, to apply a pretreatment to it and transmit it to the network to train, validate or test, is time-consuming compared to the possibility of reading all the existing images in a single file, which can be accessible via a single data group.

This Option is available by using HDF5 [19] as a unique open source technology suite for managing data collections of all sizes and complexity.

Another advantage of HDF5 is that it offers an API with multiple functions to be used to create, modify, or even delete objects throw multiple programming languages such as Python, JAVA or C++.

3.1.4. Creation of masks for cardiomegaly

The application of a supervised learning system that segments

particular information from huge datasets is a great challenge, especially in the biomedical domain where, in general, there is a lack of annotated data. That is why we created manually custom masks localizing the disease in each image. This is done by delineating the pixels corresponding to the disease areas in each image and generating a new image of the same size as the original with these pixels.

In fact, Cardiomegaly is generally easy to detect by noticing only significant thickening of the ventricular cardiac walls [20]; hence, identifying the disease area does not necessarily require high medical skills. Fig. 2 represents four examples of created masks.

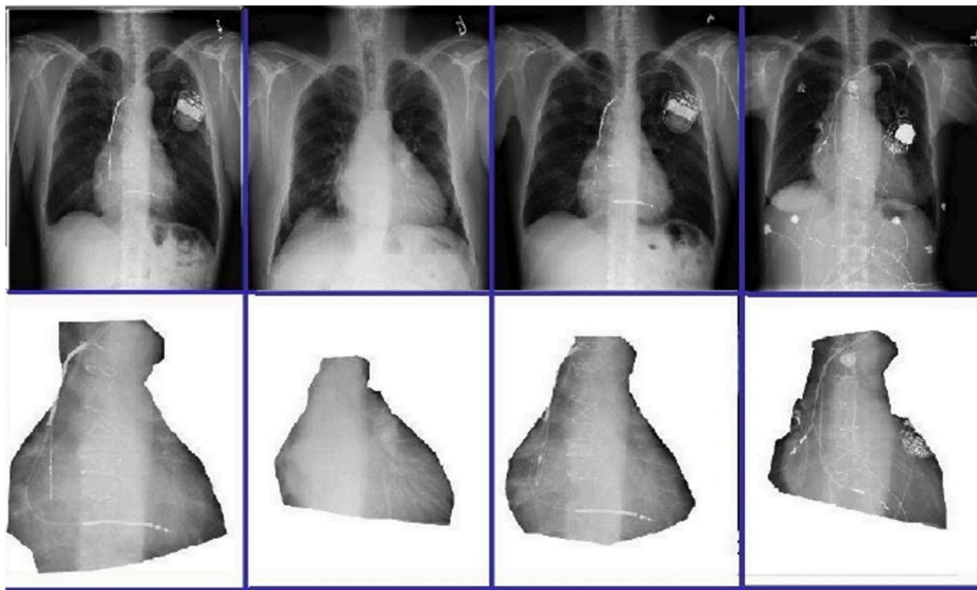


Fig. 2. Examples of four manually created masks for Cardiomegaly localization.

4. Creation of custom CNN model

4.1. Convolutional neural networks concept

In this section, we will explore the Convolutional Neural Network (CNN) and its major components. CNN is known as a powerful visual model for building intelligent systems that takes an arbitrary input image and produces a correspondingly-sized output with the most relevant information. This architecture is achieved by connecting a set of features based on pixel-to-pixel multi-layer integrity and followed by one or more fully connected layers [21] as described in Fig. 3.

CNN architecture consists of several different types of sequential layers some of which are repeated. Below we describe the most common layers:

- Input layer: represents the data entry of multiple images with standard dimension (Width x Height) with depth representation of RGB colors.
- Feature-extraction (learning) sequence: at this level, the system looks for common characteristics and ranks them in ascending order of importance. As an example of these layers we have:
 - a. Convolution layer: It consists of a set of filters that are convolved across the width and height dimensions of the image to preserve the relationship between pixels.
 - b. Pooling layer: This layer is used to reduce the number of parameters when the dataset of images is too large. Spatial pooling can reduce the dimensionality of each map but retains the important information. Spatial pooling can be of different types: Max pooling which takes the largest element from the rectified feature map, average pooling that takes the average of all elements, or sum pooling which is based on the sum of all elements.
- Classification (Fully-connected) layer: After several convolution and pooling layers, the system connects every neuron in one layer to every neuron in another layer as seen in Fig. 4.

Notice that usually we add an activation layer after the convolution layer, in order to increase the non-linearity of the network, the ReLu (Rectified Linear Unit) is an example of activation layer that is used as a common practice by researchers [22]. It is formally explained by the function $f(x) = \max(0, x)$. Also, some effective techniques, such as batch

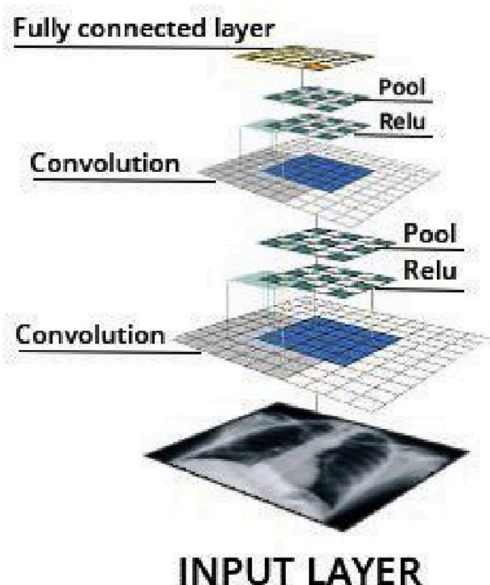


Fig. 3. CNN main components.

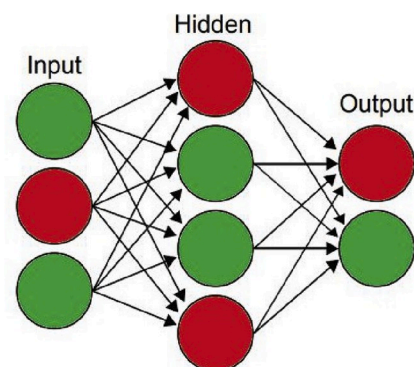


Fig. 4. Fully-connected layer.

normalization and dropout, are used to improve the performance of CNNs.

The combination between layers, batches, and normalizations leads to the birth of models with different characteristics in terms of performance, accuracy, and prediction speed that are ready for direct use like AlexNet, Microsoft COCO [23] and ImageNet [24], that provide thousands of object categories (cars, humans, cats, dogs ... etc.) in different situations for a better recognition system.

The major advantage of these preconfigured models is that, although they are created to identify objects or classify certain images, they can be used also to identify new elements. This is done by making a re-learning of last layer by passing the new elements as new data inputs, while keeping the previous layers. This operation is called fine-tuning.

As an example of these models we introduce the ALEXNET model, as mentioned in the Fig. 5 which takes a 227×227 RGB image as input, and produces a distribution over the 1000 class labels [25].

The creation of these models requires a set of collection of organized images in three main sub-datasets that are commonly used in different stages of the creation of the model.

- **Training sub-dataset:** This first category consists of pairs inputs: the image and the corresponding answer (can be: label, image or mask), which is commonly denoted as the target.
- **Validation sub-Dataset:** this sub-dataset is important in order to observe the evolution of the learning process while tuning the model's parameters.
- **Test sub-Dataset:** is an independent dataset with unlearned images used to provide an unbiased evaluation of target model fit on the first training dataset.

4.2. U-Net implementation as CNN algorithm

In May 18, 2018 the Computer Science Department of the University of Freiburg, Germany [26] suggested U-Net as new algorithm based on fully convolutional network developed for biomedical image.

The U-Net takes the position provided by the downsampling path and combine it with the contextual information in the upsampling path, to finally generate image with localization and context, which is necessary to predict a good segmentation map.

Fig. 6 gives the U-Net architecture. Generally it comprises two main parts:

- **Contracting/downsampling path:** It is similar to an encoder that capture context through compact feature map, it is composed of 4 blocks with 3×3 Convolution Layer in each block. After each Convolution Layer there exists an Activation function (with batch normalization) with 2×2 Max Pooling. It should be noted that at each pooling, the system doubles the number of feature maps, starting with 64 feature maps for the first block, 128 for the second, and so on. The reason of this contracting path comes from the input image; the system extracts the corresponding context in order to segment the image and prepare it to upsampling path through a transformation called global feature.

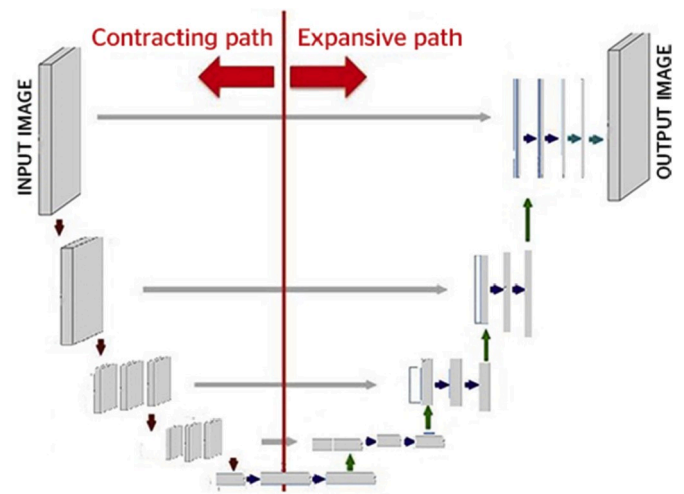


Fig. 6. U-Net downsampling/upsampling Architecture. This segmentation map is part of pixel image classification, which is made by giving label to each pixel, this labels correspond to specific class, the output of one or group of pixels is another image with good resolution and the same dimension as the original image.

- **Expanding/upsampling path:** Represents the inverse operation of the previous one. It plays the role of decoder to guarantee the good location of the cropped mask. It is composed of 4 blocks, in each of them, a deconvolution layer is concatenated with the map of the cropped characteristics coming from the subsampling stage. Between these blocks, the data that has been lost during the maximum pooling of the outsourcing stage will be reconstructed.

Another advantage of this solution is that it doesn't use any dense layer so, images of different sizes can be used as input.

5. Test conditions and results

5.1. Test environment and model parameters

To test and validate the good functioning of our proposed method we chose a special working environment. We used Kaggle as platform for data analytics using high-level neural networks API written in Python, and offering preconfigure notebook with open source datasets and GPU/CPU options. In furtherance, we used TensorFlow for the development framework as open source deep learning framework designed to numerical computation.

Our dataset of 1010 images and corresponding 1010 masks were divided into training, validation and test sub-datasets. 20% of the images were used as test data and the remaining 80% was partitioned between training (70%) and validation (10%) sets. The images were then resized to 128×128 matrix. Then the images were made available to our U-Net model. This model has multiple layers, we have fixed the model to be 35 layer deep: it starts with two 2D Convolution Layers having 3×3 as kernel size and (16,16) as filters parameters (i.e. number

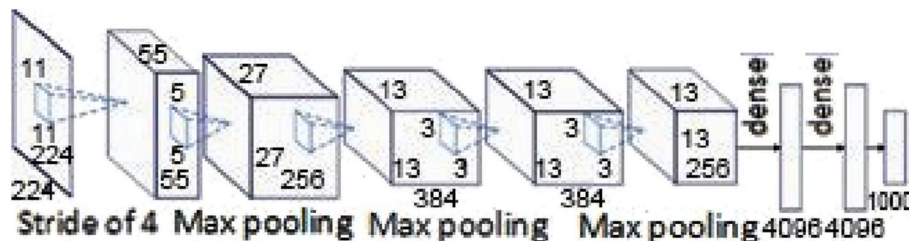


Fig. 5. ALEXNET CNN architecture.

of output filters), and ReLU as Activation Layer. After each 2D Convolution Layer we used Max pooling Layer with 2×2 as Pooling Size to reduce the size and complexity of the model. Note that we double the size of the filters after each block of (2 Conv2 and Max pooling) Layers until we reach 512, followed by a DropOut of 2%. After that we started decreasing the size of the filters on blocks until we reached the initial values of (16,16). As for the optimizer, we used ADAM (Adaptive Moment Optimization) because it works well in practice and outperforms other adaptive techniques. Fig. 7 gives a basic illustration of the layers in U-Net algorithm.

Image from the original one by gathering pixels representing the region of the disease.

5.2. Results

For any deep-learning process, the following parameters must be defined before computations:

- **Epochs:** which is the number of times for the learning process to walk through the entire dataset.
- **Batches:** An epoch is usually too big to be processed at one time by the computer, so it is divided into several smaller sets or parts, called batches.
- **Batch size:** number of training examples present in a single batch.
- **Iteration:** number of batches needed to complete one epoch.

The main interest in the process of training a neural network is to improve its performance. Once the training process is triggered, the detection accuracy gradually increases and the error rate decreases. So, we established a mechanism called EarlyStopping [35], to help us define when to optimally stop training stage. This way, we avoid overloading the network during training.

5.2.1. Cardiomegaly detection

Our computations were launched by fixing the number of epochs at 30, that of iterations at 20 and by using a batch size of.

64. The Learning/Validation rates are represented in Fig. 8 versus number of Epochs. We note a significant increase in accuracy for the two processes until values around 90% from the fifth epoch. After the tenth epoch accuracy in the validation process increases to reach values between 93% and 94% from the fifteenth epoch.

After customizing the U-Net algorithm and its 35 layers, the system was able to diagnose Cardiomegaly disease and its exact location in the CXR image. This was possible by creating new.

To make sure the obtained precision is the highest the system can achieve, we rerun the learning phase without EarlyStopping mechanism and by fixing the number of used epochs successively to 100, 120, 150 and 200. As we can see in Table 1, the learning accuracy decreases as the number of epochs used increases.

5.2.2. Cardiomegaly localization

After extracting Cardiomegaly images, creating a custom mask for each image and compressing the new dataset using HDF5, the U-Net model was able to localize the disease in test images (20% of full

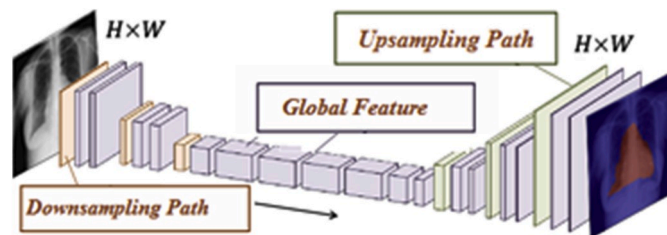


Fig. 7. U-Net order layers implementation.

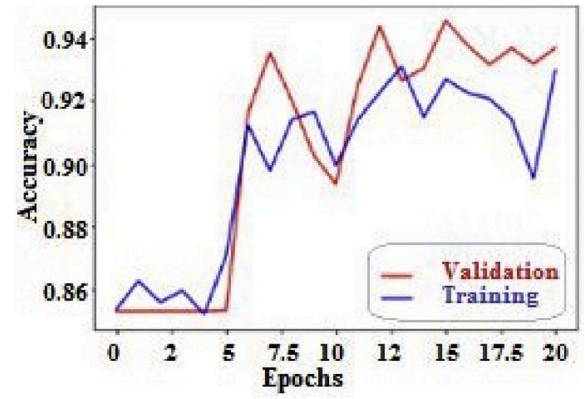


Fig. 8. Evolution of learning/validation process accuracy.

Table 1

Validation accuracy versus number of epochs.

Epochs	Training/Validation accuracy (%)
100	87.3
120	86.4
150	85.0
200	71.9

dataset). Fig. 9 represents four generated images showing Cardiomegaly localization.

5.2.3. Discussion

Owing to our customized U-Net based CNN model a high accuracy of detection between 93 and 94% was possible, which is greater than previously published results for Chest Pathology Identification; namely [10], which used preconfigured and heavy models such as ResNet-101, to achieve an accuracy of 92%, or [11] that used a large MIMIC-CXR dataset (thousands of images) to reach an accuracy of 91% or even [13], where the accuracy was only 89%.

This method was tested on Cardiomegaly, but it can be used to detect and localize the seven other remaining diseases in the X-ray8 database. Nevertheless, this requires the integration of radiologists and physicians to set up the proper masks of each disease, and also to validate the obtained results.

6. Conclusion

In this work, we presented a complete process to automatically detect Cardiomegaly disease from X-Ray images. We relied on X-ray images that were obtained from the Chest Xray-8 dataset. The process is achieved in four steps starting with the extraction of Cardiomegaly images from Chest Xray-8 dataset. In the second step we improved the quality of extracted images by applying the method of Adaptive Histogram Equalization (LC-AHE). In a third step, we compressed images to enhance the processing speed using HDF5. The fourth and final step was dedicated to data processing via a customized CNN model based on U-Net.

Accordingly, we obtained an accuracy between 93 and 94% for detecting Cardiomegaly, which is at the time of this article being written the highest percentage reported in the literature. We can say also that this work is the first one where deep learning methods were tested for the detection of thoracic pathologies using the U-Net algorithm, especially with a learning phase based on non-medical archive. In addition, with U-Net, precise localization of Cardiomegaly is possible, which is not the case for the previous works. Finally, the proposed model can be applied in a generic way to detect other thoracic pathologies.

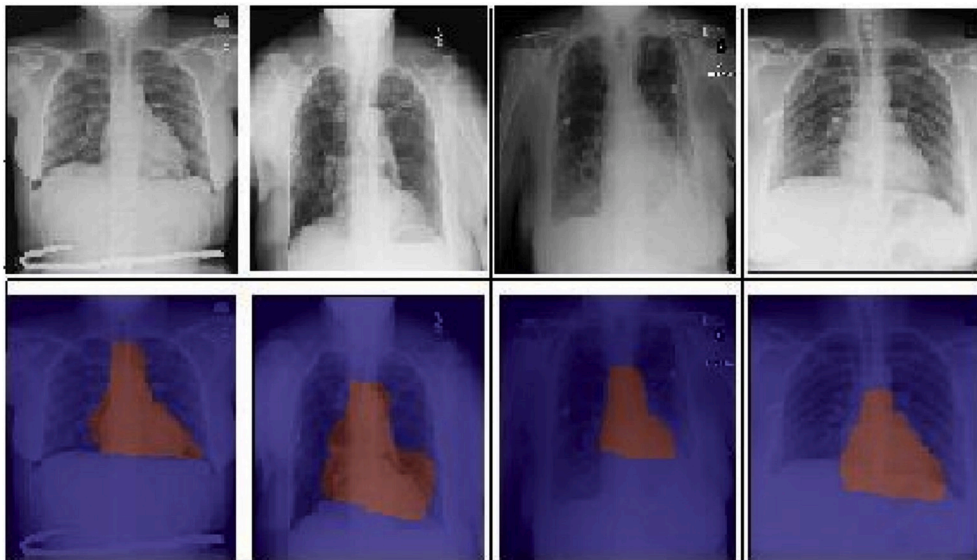


Fig. 9. Four examples of Cardiomegaly localization disease using U-Net. Original figures (up), generated images showing disease localization (down).

Ethical statement

The authors whose names are listed in the end of the document certify that they have NO affiliations with or involvement in any organization or entity with any financial interest (such as honoraria; educational grants; participation in speakers' bureaus; membership, employment, consultancies, stock ownership, or other equity interest; and expert testimony or patent-licensing arrangements), or non-financial interest (such as personal or professional relationships, affiliations, knowledge or beliefs) in the subject matter or materials discussed in this manuscript.

Also The authors confirm that the manuscript has no actual or potential conflict of interest with any party, including but not limited to any financial, personal or other relationship with other people or organization within three years of beginning the submitted work that could inappropriately influence or be perceived to influence. We confirm that the paper has not been published previously, is not under consideration for publication elsewhere, and is not being simultaneously submitted elsewhere.

Declaration of competing interest

None.

Acknowledgement

We thank our teacher's **Dr. Yassin Laaziz** and **Dr. Abdelhak Tali** who provided insight and expertise that greatly assisted the research.

We thank also "Department of Radiology and Imaging Sciences, Clinical Center, 2 National Center for Biotechnology Information, National Library of Medicine" for sharing their rich Dataset with community.

We would also like to show our gratitude to the **Edward J Ciaccio, Farooqui, Mehroon Nesa, and Achuthan, Arivalagan** for their supports with us during the course of this research, and we thank EVISE reviewers for their interesting comments, although any errors are our own and should not tarnish the reputations of these esteemed persons.

References

- [1] Zhong-Qiu Z, Zheng P, Shou-tao X, Wu X. Object detection with deep learning: A review, vol. 14; 8, MARCH 2017. from, <https://arxiv.org/pdf/1807.05511.pdf>.
- [2] B.Mihai-Sorin, F. Iulian-Ionuț, F. Laura, Constantin Vertan, "The use of deep learning in image segmentation, classification and detection", The image processing and analysis lab (LAPI), Politehnica University of Bucharest, Romania, from <https://arxiv.org/pdf/1605.09612.pdf>.
- [3] Bush Isabel. Stanford computer science, 353 serra mall. Stanford, CA: Lung Nodule Detection and Classification; 2016. p. 94305. from, http://cs231n.stanford.edu/reports/2016/pdfs/313_Report.pdf.
- [4] Candemir Sema, Jaeger Stefan, Karagyris Alexandros, KC Santosh, Vajda Szilárd, Xue Zhiyun. In: Automated detection of lung diseases in chest X-rays. Medical Science & Computing, Inc; 2015. from, <https://lhncbc.nlm.nih.gov/system/file/s/pub9126.pdf>.
- [5] Lakhani Paras, Sundaram Baskaran. Deep learning at chest radiography: automated classification of pulmonary tuberculosis by using convolutional neural networks, vol. 284; 2 August 2017. from, <https://arxiv.org/pdf/1705.09850.pdf>.
- [6] Rajpurkar Pranav, Irvin Jeremy, Zhu Kaylie, Yang Brandon, Mehta Hershel, Duan Tony, Ding Daisy, Bagul Aarti, Ball Robyn L, Langlotz Curtis, Shpanskaya Katie, Lungren Matthew P, Ng Andrew Y. CheXNet: radiologist-level Pneumonia detection on chest X-rays with deep learning. from, <https://arxiv.org/pdf/1711.05225.pdf>; 25 Dec 2017.
- [7] Wang Xiaosong, Peng Yifan, Lu Le, Lu Zhiyong, Bagheri Mohammad hadi, Summers Ronald M, Department of Radiology and Imaging Sciences, Clinical Center, 2 National Center for Biotechnology Information, National Library of Medicine, National Institutes of Health, Bethesda. ChestX-ray8: hospital-scale chest X-ray database and benchmarks on weakly-supervised classification and localization of common thorax diseases. from, <https://arxiv.org/pdf/1705.02315.pdf>.
- [8] Etta Pisano, Bradley M. Hemminger, Shuquan Zong, Stephen M. Pizer, "Contrast Limited Adaptive Histogram Equalization image processing to improve the detection of simulated spiculations in dense mammograms", DOI: 10.1007/BF03178082..
- [9] Ronneberger Olaf, Fischer Philipp, Brox Thomas, Computer Science Department and BIOS Centre for Biological Signalling Studies, University of Freiburg, Germany. U-Net: convolutional networks for biomedical image segmentation. from: <https://arxiv.org/pdf/1505.04597.pdf>; 18 May 2015.
- [10] Bar Y, Diamant I, Wolf L, Greenspan H. Deep learning with non-medical training used for chest pathology identification. In: Proceedings of SPIE medical imaging. Orlando, FL, USA: International Society for Optics and Photonics; February 2015. 94140V.
- [11] Rubin Jonathan, Sanghavi Deepan, Zhao Claire, Lee Kathy, Qadir Ashequl, Xu-Wilso Minnan. Large scale Automated reading of frontal and lateral chest X-rays using dual convolutional neural networks. from: <https://arxiv.org/pdf/1804.07839.pdf>; 24 Apr 2018.
- [12] Mohammad Tariqul Islam1, Md Abdul Aowal1, Ahmed Tahseen Minhaz1, Khalid Ashraf2 1Semion, House 167, Road 3, Mohakhali DOHS, Dhaka, Bangladesh, "Abnormality Detection and Localization in Chest X-Rays using Deep Convolutional Neural Networks", 2Semion, 1811 Francisco St, St 2, Berkeley, CA 94703, USA, from : <https://arxiv.org/pdf/1705.09850.pdf>.
- [13] Bar Yaniv, Diamant Idit, Wolf Lior, Lieberman Sivan, Konen Eli, Greenspan Hayit. Chest pathology identification using deep feature selection with non-medical training. from, https://www.cs.tau.ac.il/~wolf/papers/chest_miccai2015.pdf. <https://doi.org/10.1155/2017/2727686>.
- [14] Tataru Christine, Yi Darwin, Shenoyas Archana, Ma Anthony. Deep Learning for abnormality detection in Chest X-Ray images. from, <http://cs231n.stanford.edu/reports/2017/pdfs/527.pdf>; June, 13, 2017.

- [15] Ren Ning-ning, Ma An-ran, Han Li-bo, Sun Yong, Shao Yan, Qiu Jian-feng. Automatic radiographic position recognition from image frequency and intensity. *J Healthcare Eng* 2017;2727686.
- [16] Zhu Youlian, Huang Cheng. An adaptive histogram equalization algorithm on the image gray level mapping. In: *International conference on solid state devices and materials science*; 2012.
- [17] Stephen M. Pizer, R. Eugene Johnston, James P. Ericksen, Bonnie C. Yankaskas, Keith E. Muller, Medical image Display research group university of North Carolina, "Contrast Ltd Adapt Histogram Equal: Speed Effect", from <http://www.cs.unc.edu/techreports/90-035.pdf>.
- [18] Haller Elisabeta Antonia. Adaptive histogram equalization in GIS. *Ann Univ Craiova - Math Comput Sci Ser* 2011;38(1). ISSN: 1223-6934:100–4.
- [19] HDF5 team. High level introduction to HDF5. from, <https://support.hdfgroup.org/HDF5/Tutor/HDF5Intro.pdf>; September 23, 2016.
- [20] M. Ilovar and L.Šajn, Faculty of computer and information science, Ljubljana, Slovenia, "Anal Radiogr Detect Cardiomegaly", from https://www.researchgate.net/publication/221413003_Analysis_of_radiograph_and_detection_of_cardiomegaly.
- [21] Thoma Martin. Department of computer science institute for anthropomatics and FZI research center for information technology. *Anal Optim Conv Neural Net Arch* 31 Jul 2017. 1707.09725v1.
- [22] Ramachandran Prajit, Zoph Barret, Le Quoc V. Searching for activation functions. from, 1710.05941v2; 27 Oct 2017. <https://arxiv.org/pdf/1710.05941.pdf>.
- [23] Tsung-Yi L, Maire M, Belongie S, Bourdev L, Girshick R, Hays J, Perona P, Ramanan D, Lawrence Zitnick C, Dollar P. Microsoft COCO: common objects in context. from, <https://arxiv.org/pdf/1405.0312.pdf>.
- [24] Long Jonathan, Shelhamer Evan, Darrell Trevor, UC Berkeley. Fully convolutional networks for semantic segmentation. from, 1411.4038v2; 8 Mar 2015. <https://arxiv.org/pdf/1411.4038.pdf>.
- [25] Krizhevsky A, Sutskever I, Hinton E. ImageNet classification with deep convolutional neural networks. from: <https://www.nvidia.cn/content/tesla/pdf/machine-learning/imagenet-classification-with-deep-convolutional-nn.pdf>.
- [26] Ronneberger Olaf, Fischer Philipp, Brox Thomas, Computer Science Department and BIOSS Centre for Biological Signalling Studies, University of Freiburg, Germany. U-Net: convolutional networks for biomedical image segmentation. 1505.04597v1; 18 May 2015. <https://arxiv.org/pdf/1505.04597.pdf>.